High power vertical-external-cavity surface-emitting laser

Peng Zhang (张 鹏)[1], Yanrong Song (宋晏蓉)[1*], Xinping Zhang (张新平)[1], Jinrong Tian (田金荣)[1], and Zhigang Zhang (张志刚)[2]

[1]*College of Applied Sciences, Beijing University of Technology, Beijing 100124, China*

[2]*School of Electronics Engineering and Computer Science, Peking University, Beijing 100871, China*

[*]*E-mail: yrsong@bjut.edu.cn*

Received August 10, 2009

A high power optically-pumped vertical-external-cavity surface-emitting laser with a diamond heatspreader is demonstrated. Owing to the good thermal conductivity, diamond can accelerate the dissipation of heat in the active region and increase the output power significantly. The effects of the curvature radius, the transmission of output coupler, the spot size of the pump, and the temperature of the heat sink on the output power are investigated. A maximum output power of 880 mW is obtained under the conditions of 10 °C temperature, 15-mm curvature radius, 3% transmission of the output coupler, and 8500-mW pump power. The slope efficiency and the optical-to-optical conversion efficiency of the laser are about 17% and 15%, respectively.

OCIS codes: 140.0140, 140.3460, 140.3480, 140.5960.

doi: 10.3788/COL20100804.0401.

Optically pumped vertical-external-cavity surface-emitting lasers (VECSELs), or known as semiconductor disk lasers (SDLs), combine the advantages of both the surface-emitting lasers and disk lasers. Their wavelength covers from visible to infrared band[1,2]. Besides the high output power and high beam quality[3−5], the adjustable external cavity of the VECSEL allows convenient insertion of optical elements. For example, a nonlinear crystal can be introduced for frequency conversion[6−8], a saturable absorption mirror can be inserted for passive mode-locking[9], and a spectral filter can be put in for single-frequency operation or wavelength tuning[10].

The VECSELs have many advantages for power scalability. Firstly, optical pump can provide controlled and uniform distribution of the pump power over the active region, so the above-gap absorption through barrier material is more efficient and less sensitive to the deviation of pump wavelength. Secondly, the undoped active region means absence of the free carrier absorption, that is, the less energy loss and heat deposition. Finally, the active region in gain chip is cooled by a quasi-one-dimensional heat flow and the related thermal gradient is along the axis of the optical cavity, so the problems associated with thermal lens and depolarization are minimized[11].

The limitation for the output power of a VECSEL comes from its heat problem. With the temperature increasing, the gain of the quantum wells (QWs) will decrease sharply[12], the redshift of the laser wavelength will detune the periodic resonant gain (PRG) structure, and the nonradiative recombination will become dominant[13]. All of the above factors are compounded until finally the thermal rollover of the laser occurs and the device stops lasing.

The two kinds of technology introduced in the thermal management of VECSEL are substrate removal[3] and use of heatspreader[14]. In the former method, the wafer should grow following a reverted sequence (i.e., firstly the etch-stop layers on the substrate, then the cap layer, the window layer, the QWs, and finally the distributed Bragg reflector (DBR)). Then the divided chip is soldered DBR-side down on the heat sink and the substrate can be removed by chemical etching. Here we use the latter process. The high thermal conductivity up to 20 W/(cm·K) and the good transparency for 1-μm waveband make diamond an ideal material as the heatspreader of the VECSEL operating around 1-μm wavelength. A 3×3×0.3 (mm) chip of chemical vapor deposited diamond heatspreader is bonded to the gain chip using the method of liquid capillary bonding[15].

In this letter, we present a high power VECSEL with a diamond heatspreader. The experimental setup and the epitaxial structure of the semiconductor wafer are shown in Fig. 1. In the epitaxial structure, the DBR contained 30 pairs of alternating GaAs and AlAs layers; the active region consisted of 16 non-compensated compressively strained $In_{0.20}Ga_{0.80}As$ QWs which were spaced by the $Al_{0.05}GaAs$ barriers and located at the antinodes of the standing wave of the laser in the microcavity to form the PRG structure[16]. An $Al_{0.6}GaAs$ layer, which was transparent for the oscillation laser and the pump laser, provided a high barrier as the window layer and a GaAs cap layer was used to finish the growth. In the experimental setup, a 2×2 (mm) gain chip was bonded to a copper heat sink which was temperature controlled by a Peltier cooler. The back plate of the entire device was water-cooled. An 808-nm pump radiation was collimated and focused on the semiconductor disk at an angle of about 45°, and the diameter of the pump spot was approximately 100 μm (except there was a special explanation). A plane-concave mirror was used as the output coupler.

Figure 2 shows the output power with and without heatspreader under conditions of 25-mm curvature radius, 3% transmission, and 10 °C heat sink temperature. The maximum output power of VECSEL without diamond heatspreader is 196 mW and further increase of pump power will result in the output falling, while the maximum output of VECSEL with a diamond heatspreader is up to 710 mW, which is about 2.5 times more than the former. As shown in Fig. 2, the diamond heat-

spreader can improve the heat dissipation and upgrade the output power significantly. However, the introduced additional loss of the diamond heatspreader increases the lasing threshold and decreases the slope efficiency (SE) at the same time.

Output power of VECSELs with different curvature radii of the external coupler is shown in Fig. 3, the transmission of the coupler is 3% and the temperature of the heat sink is 0 °C. The inset of Fig. 3 shows the diameter of laser spot on the gain chip versus the cavity length. As can be seen from the inset, the laser with 15-mm coupler satisfies the mode-matched condition at point A, while the laser with 25-mm coupler satisfies at point B, and the former satisfies the mode-matched

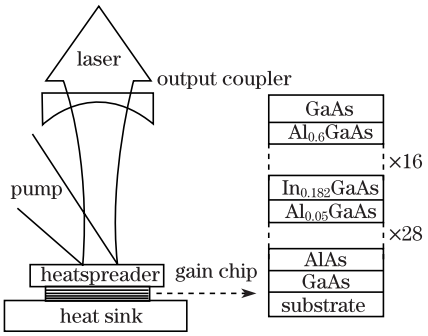

Fig. 1. Schematic of the VECSEL (left) and epitaxial structure of the semiconductor wafer (right).

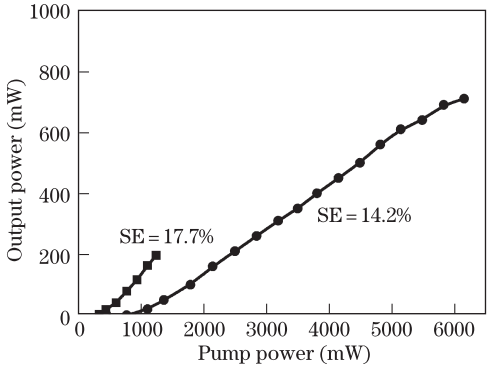

Fig. 2. Output power of the laser with (circle) and without (square) the heatspreader. $R_{\rm OC}$ = 25 mm, $T_{\rm OC}$ = 3%, and $T_{\rm heat\ sink}$ = 10 °C.

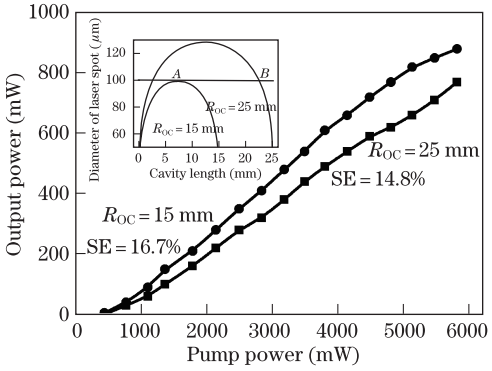

Fig. 3. Effect of the curvature radius of external coupler on the output power. The inset shows the diameter of laser spot on gain chip versus the cavity length. $T_{\rm OC}$ = 3% and $T_{\rm heat\ sink}$ = 0 °C.

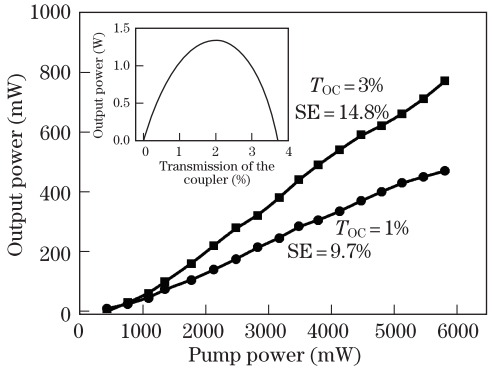

Fig. 4. Output power of VECSELs with different transmission of the external mirror. The inset shows the theoretical dependence of output power on the transmission of the external coupler under 6-W pump power. $R_{\rm OC}$ = 25 mm and $T_{\rm heat\ sink}$ = 0 °C.

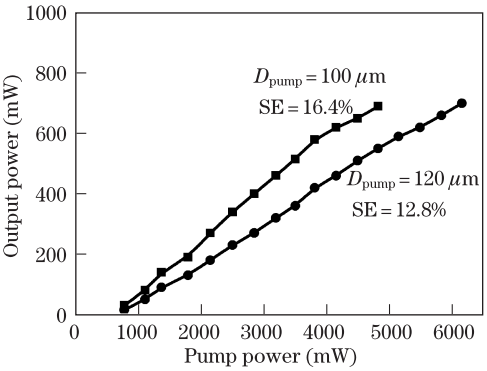

Fig. 5. Influence of the pump spot on the output power. $R_{\rm OC}$ = 15 mm, $T_{\rm OC}$ = 3%, and $T_{\rm heat\ sink}$ = 10 °C.

condition better than the latter. The maximum output power and SE for the laser with 15-mm curvature radius mirror are 880 mW and 16.7%, respectively, while they are 770 mW and 14.8% for the laser with 25-mm curvature radius mirror.

The output power as a function of pump power for VECSELs with different transmission of the end mirror is plotted in Fig. 4, and the theoretical dependence of the output power on the transmission of the coupler is also plotted as an inset. It is obvious that the laser with 3% transmission mirror has bigger threshold and higher SE compared with the laser with 1% transmission mirror. It can be concluded from the inset that the optimum transmission of the coupler is about 2%. Since we have no sufficient mirrors with various transmissions, the optimum transmission of the mirror for the laser is not obtained experimentally, and this work can be done in the future.

The influence of the pump spot on the output power can be seen from Fig. 5. When the diameter of the pump spot is 100 μm, the laser output begins to reduce after reaching 690 mW because of the thermal effect. But when the diameter of the pump spot is enlarged to 120 μm, no output falling is observed under the pump power we can afford. It is clear that expanding pump spot can help the dissipation of the heat, hold back the power falling and enhance the output power, although it will raise the threshold and lower the SE of the laser.

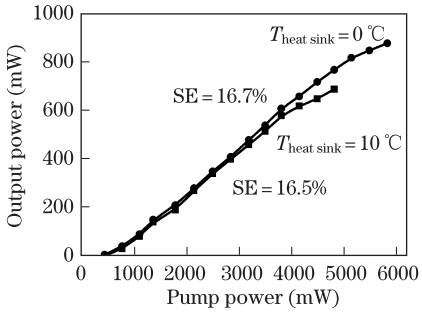

Fig. 6. Output power of the lasers under different temperatures of the heat sink. $R_{OC} = 15$ mm and $T_{OC} = 3\%$.

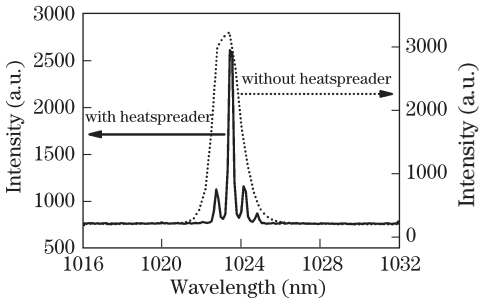

Fig. 7. Lasing spectra of VECSELs with (solid line) and without (dot line) the heatspreader.

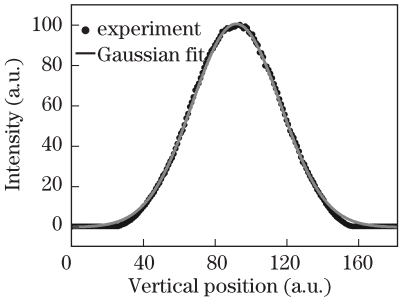

Fig. 8. Far-field distribution of the beam intensity.

Figure 6 shows the effect of the temperature of heat sink on the output power. The output of the laser under 10 °C heat sink temperature begins to decrease after touching 690 mW. When the temperature is reduced to 0 °C, the maximum output can be up to 880 mW. Figure 6 indicates that VECSEL with lower heat sink temperature has higher output power.

The laser spectra with and without the heatspreader are drawn together in Fig. 7. As can be seen, when the heatspreader is not present on the gain chip, the laser spectrum is located at 1023 nm with a linewidth (full-width at half-maximum (FWHM)) of about 2 nm. After the heat spreader is bonded on the gain chip, there are four identifiable longitudinal modes in the laser spectrum and the space of the adjacent longitudinal mode is about 0.7 nm, which is corresponding to the mode space of a 0.3-mm-thick diamond etalon at 1023 nm. The other effects of a diamond heat spreader in a VECSEL can be found in Ref. [17].

Figure 8 shows the ideal Gaussian distribution of the laser beam intensity. The measured M^2 factor of the output beam is about 1.07, which demonstrates a near diffraction-limited good beam quality.

In conclusion, we have demonstrated a high power VECSEL with a diamond heatspreader. Although the diamond heatspreader will bring additional loss, increase the lasing threshold, decrease the SE, and bring up the etalon effect, its excellent thermal conductivity can improve the heat dissipation in the active region, retard the power falling, and upgrade the maximum output power significantly. The output power of the laser can also be increased in a certain extent by means such as enlarging the pump spot, decreasing the curvature radius of the end mirror, increasing the transmission of the coupler properly, or reducing the temperature of the heat sink. 880-mW output power is obtained using an external coupler with 15-mm curvature radius and 3% transmission under 6500-mW pump power and 0 °C heat sink temperature. By further improving the wafer growth, along with substrate removing, we believe that multi-watts even tens of watts of output power can be realized.

The authors would like to thank C. Jagadish and Hark Hoe Tan for providing the semiconductor wafer. This work was supported by the National Natural Science Foundation of China under Grant No. 60678010.

References

1. J. E. Hastie, L. G. Morton, S. Calvez, M. D. Dawson, T. Leinonen, M. Pessa, G. Gibson, and M. J. Padgett, Opt. Express **13,** 7209 (2005).
2. J. M. Hopkins, N. Hempler, B. Rösener, N. Schulz, M. Rattunde, C. Manz, K. Köhler, J. Wagner, and D. Burns, Opt. Lett. **33,** 201 (2008).
3. M. Kuznetsov, F. Hakimi, R. Sprague, and A. Mooradian, IEEE J. Sel. Top. Quantum Electron. **5,** 561 (1999).
4. A. C. Tropper and S. Hoogland, Prog. Quantum Electron. **30,** 1 (2006).
5. Y. Zhou, D. Zhao, Y. Li, and Q. Yang, Chin. Opt. Lett. **6,** 855 (2008).
6. A. J. Maclean, A. J. Kemp, S. Calvez, J. Y. Kim, T. Kim, M. D. Dawson, and D. Burns, IEEE J. Quantum Electron. **44,** 216 (2008).
7. Y. Song, P. Zhang, X. Zhang, B. Yan, Y. Zhou, Y. Bi, and Z. Zhang, Chin. Opt. Lett. **6,** 271 (2008).
8. Y. Song, P. Zhang, B. Yan, Y. Zhou, Y. Bi, and Z. Zhang, Chinese J. Lasers (in Chinese) **34,** 1736 (2007).
9. P. Klopp, F. Saas, M. Zorn, M. Weyers, and U. Griebner, Opt. Express **16,** 5770 (2008).
10. F. Li, M. Fallahi, J. T. Murray, R. Bedford, Y. Kaneda, A. R. Zakharian, J. Hader, J. V. Moloney, W. Stolz, and S. W. Koch, Appl. Phys. Lett. **88,** 021105 (2006).
11. A. C. Tropper, H. D. Foreman, A. Garnache, K. G. Wilcox, and S. H. Hoogland, J. Phys. D Appl. Phys. **37,** R75 (2004).
12. P. Zhang, Y. Song, J. Tian, X. Zhang, and Z. Zhang, J. Appl. Phys. **105,** 053103 (2009).
13. J. Hader, J. V. Moloney, and S. W. Koch, IEEE J. Quantum Electron. **41,** 1217 (2005).
14. W. J. Alford, T. D. Raymond, and A. A. Allerman, J. Opt. Soc. Am. B **19,** 663 (2002).
15. Z. L. Liau, Appl. Phys. Lett. **77,** 651 (2000).
16. S. W. Corzine, R. S. Geels, J. W. Scott, R. H. Yan, and L. A. Coldren, IEEE J. Quantum Electron. **25,** 1513 (1989).
17. F. Loon, A. J. Kemp, A. J. Maclean, S. Calvez, J. M. Hopkins, J. E. Hastie, M. D. Dawson, and D. Burns, Opt. Express **14,** 9250 (2006).